STRUCTURAL SCIENCE
CRYSTAL ENGINEERING
MATERIALS

Volume 74 (2018)

Supporting information for article:

Control of crystal structure using temperature and time

Savannah C. Zacharias, Gaëlle Ramon and Susan A. Bourne

S1 Thermal analysis

Table S1: Theoretical and experimentally obtained mass losses of **I**, **II**, and **III**. The components are given in the order in which they are lost

	Component	**Mass loss [%] (calculated)**	**Mass loss [%] (observed)**
I	$\mathbf{[Fe(C_5H_7O_2)(C_7H_3N_1O_4)(H_2O)]\cdot C_2H_3N}$		
	Acetonitrile	10.8	10.7 ± 0.3
	Water	4.7	3.8 ± 0.6
	Acetylacetonate	26.4	20.4 ± 0.4 partial
	2,6-pyridinedicarboxylic acid	43.6	23.4 ± 0.4 partial
	Fe(III)	14.4	
	FeO_4	31.6	
II	$\mathbf{Fe(C_5H_7O_2)(C_7H_3NO_4)}$		
	Acetylacetonate	31.3	32.7 ± 0.4
	2,6-pyridinedicarboxylic acid	51.6	30.9 ± 1.1 partial
	Fe(III)	17.3	
	FeO_4	37.5	
III	$\mathbf{[Fe(C_5H_7O_2)(C_7H_3NO_4)]_4}$		
	Acetylacetonate	31.3	31.2 ± 2.4
	2,6-pyridinedicarboxylic acid	51.6	26.2 ± 1.2 partial
	Fe(III)	17.3	
	FeO_4	37.5	

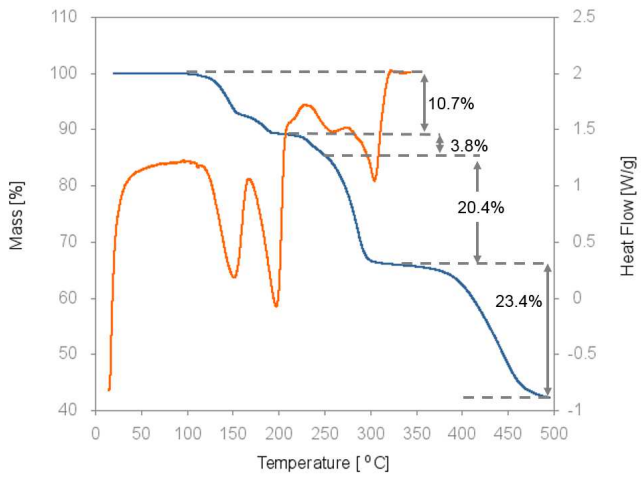

Figure S1: Overlay of TGA and DSC traces of **I**. The sequential loss of acetonitrile, water, acetylacetonate, 2,6-pyridinedicarboxylic acid is shown.

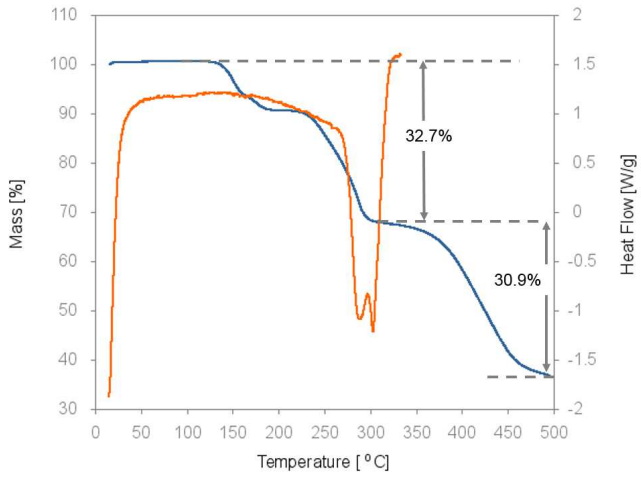

Figure S2: The complex multistep loss of acetylacetnoate followed by the partial loss of 2,6-pyridinedicarboxylic acid can be seen in the overlay of TGA and DSC traces of **II**.

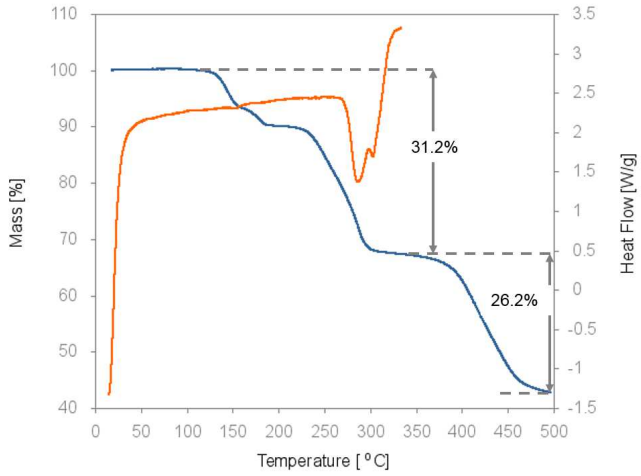

Figure S3: Overlay of TGA and DSC traces of **III** showing the complex degradation of acetylacetonate followed by the partial loss of 2,6-pyridinedicarboxylic acid.

S2 X-ray diffraction (XRD)

Powder X-diffraction patterns of **I**, **II**, and **III**.

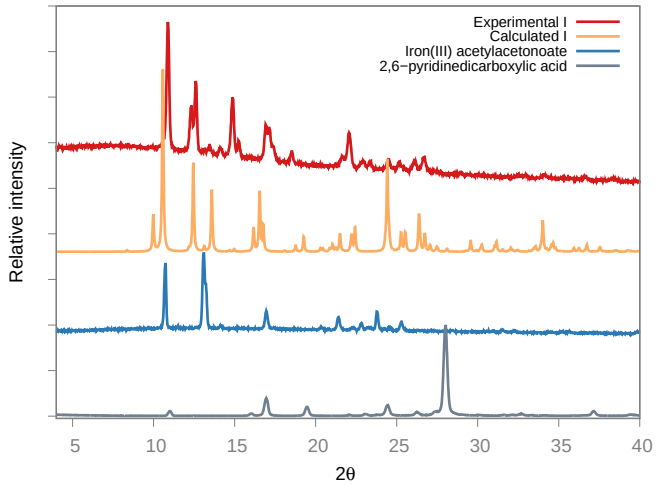

Figure S4: PXRD trace of **I** and starting materials. There is partial agreement between the experimental and calculated traces, indicating that the bulk material may be a mixture of compounds.

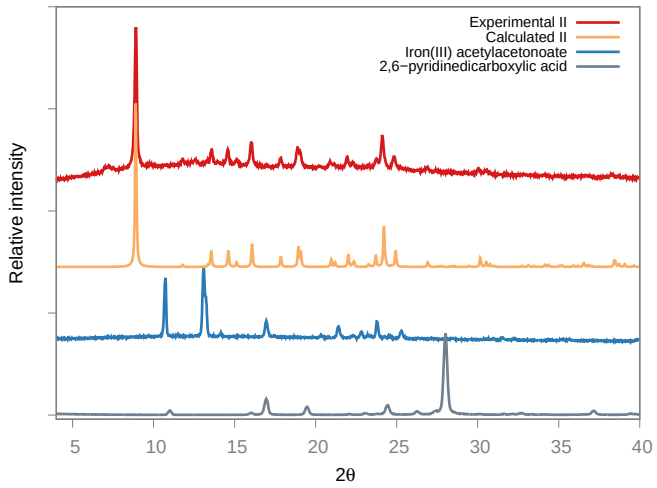

Figure S5: PXRD trace of **II** and starting materials. A new phase has formed and there is good agreement between the experimental and calculated patterns.

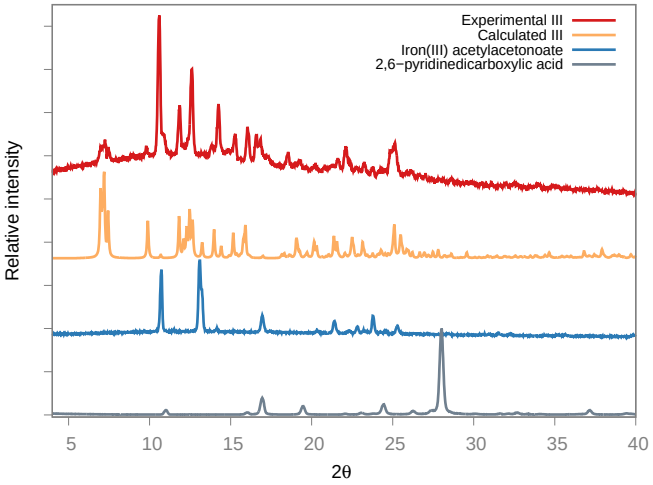

Figure S6: PXRD trace of **III** and starting materials. A new phase is present but some discrepancy between the experimental and calculated patterns may indicate that the phase is not pure.

S2.1 Crystal structures of I, ZIMBIG, II, and III

S2.2 I

Table S2: Bond lengths and angles of atoms coordinated to the Fe(III) metal centre of **I**

Bond	**Length** [Å]	**Bonds**	**Angle** [°]
Fe1−O1	2.033(1)	N1−Fe1−O6	88.94(5)
Fe1−O4	2.034(1)	N1−Fe1−O7	94.09(5)
Fe1−O5	1.929(1)	O4−Fe1−O5	104.07(5)
Fe1−O6	1.998(1)	O5−Fe1−O1	104.56(5)
Fe1−O7	2.032(1)	N1−Fe1−O1	75.51(5)
Fe1−N1	2.068(1)	O4−Fe1−N1	75.95(5)

S2.3 ZIMBIG

Figure S7: Asymmetric unit of ZIMBIG showing coordination to Fe(III) metal centre and the disordered ethanol molecule (Lainé *et al.*, 1995b).

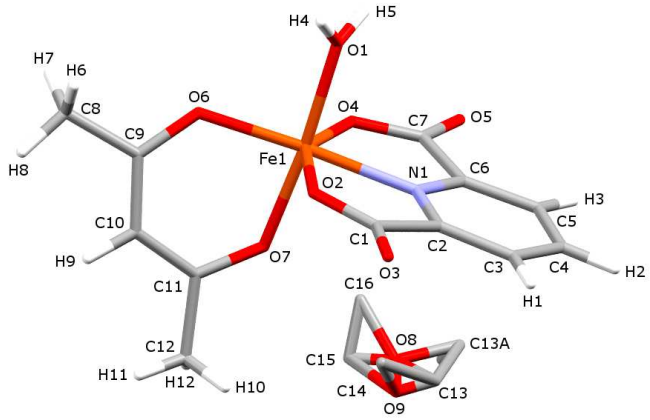

Table S3: Summary of bond lengths and angles of atoms coordinated to the Fe(III) metal centre of ZIMBIG

Bond	**Length [Å]**	**Bonds**	**Angle [°]**
Fe1−O1	2.002(2)	N1−Fe1−O7	92.16(9)
Fe1−O2	2.046(2)	N1−Fe1−O1	92.80(8)
Fe1−O4	2.035(2)	O4−Fe1−O6	111.64(9)
Fe1−O6	1.936(3)	O4−Fe1−O2	97.26(9)
Fe1−O7	1.977(2)	N1−Fe1−O2	75.42(7)
Fe1−N1	2.069(2)	O4−Fe1−N1	74.69(7)

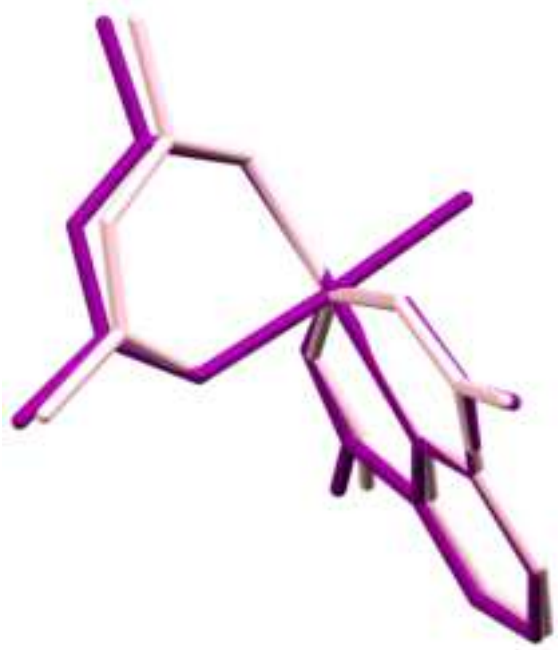

Figure S8: The root mean square deviation fit of the asymmetric units of ZIMBIG (Lainé *et al.*, 1995) (pink) and **I** (purple). Hydrogen atoms and solvent molecules were omitted for clarity. RMSD fit between the two molecules is 0.093 Å.

Figure S9: Packing of ZIMBIG viewed down [100] on the left and [010] on the right (Lainé *et al.*, 1995b). Hydrogen atoms and ethanol solvent molecule are omitted for clarity. The disordered ethanol molecule can be found in a channel propagating along [010]. This packing arrangement is different to that seen for **I** (Fig. **??**).

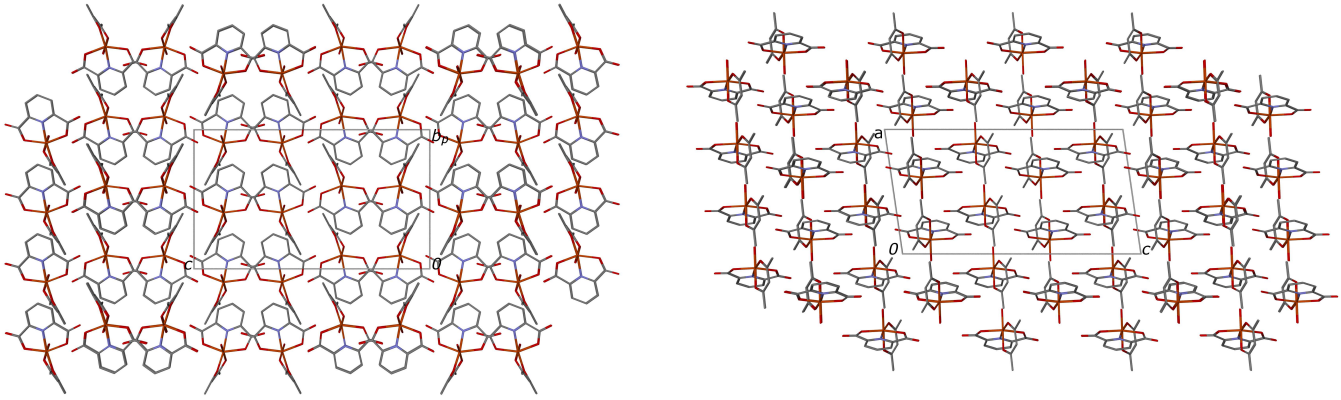

S2.4 II and III

Table S4: Coordination geometry of the ligands to the metal centre of **II**

Bond	**Length [Å]**	**Bond**	**Angle [°]**
Fe1−O3	1.9891(2)	O3−Fe1−N1	76.52
Fe1−O2	2.0864(2)	O2−Fe1−N1	74.60
Fe1−O5	1.9406(2)	O6−Fe1−N1	88.87
Fe1−O6	1.9817(2)	O5−Fe1−O6	88.06
Fe1−N1	2.0764(2)	O5−Fe1−O1a	86.60
Fe1−O1a	2.0409(2)	N1−Fe1−O1a	97.70

Table S5: Coordination geometry, bond lengths, of the ligands to the metal centre of **III**

Bond	**Length** [Å]	**Bond**	**Length** [Å]	**Bond**	**Length** [Å]	**Bond**	**Length** [Å]
Fe1A−O1D	2.0286(1)	Fe1B−O1A	2.0603(1)	Fe1C−O1B	2.0477(1)	Fe1D−O1C	2.0596(1)
Fe1A−O2A	2.0959(1)	Fe1B−O2B	2.0728(1)	Fe1C−O2C	2.0936(1)	Fe1D−O2D	2.0988(1)
Fe1A−O3A	1.9776(1)	Fe1B−O3B	2.0089(1)	Fe1C−O3C	1.9870(1)	Fe1D−O3D	2.0026(1)
Fe1A−O5A	1.9925(1)	Fe1B−O5B	1.9927(1)	Fe1C−O5C	1.9906(1)	Fe1D−O5D	1.9873(1)
Fe1A−O6A	1.9569(1)	Fe1B−O6B	1.9295(1)	Fe1C−O6C	1.9577(1)	Fe1D−O6D	1.9445(1)
Fe1A−N1A	2.0903(1)	Fe1B−N1B	2.0814(1)	Fe1C−N1C	2.0983(1)	Fe1D−N1D	2.0762(1)

Table S6: Coordination geometry, bond angles, of the ligands to the metal centre of **III**

Bond	**Angle** [°]	**Bond**	**Angle** [°]
O2A−Fe1A−N1A	73.72(1)	O2B−Fe1B−N1B	74.97(1)
O1D−Fe1A−N1A	96.69(1)	O1A−Fe1B−N1B	96.81(1)
O5A−Fe1A−O6A	87.56(1)	O5B−Fe1B−O6B	88.27(1)
O2A−Fe1A−O5A	86.60(1)	O2B−Fe1B−O5B	91.72(1)
O3A−Fe1A−N1A	76.29(1)	O3B−Fe1B−N1B	76.43(1)
O1D−Fe1A−O3A	95.62(1)	O1A−Fe1B−O3B	91.83(1)
O2C−Fe1C−N1C	73.71(1)	O2D−Fe1D−N1D	74.78(1)
O1B−Fe1C−N1C	100.78(1)	O1C−Fe1D−N1D	98.18(1)
O5C−Fe1C−O6C	87.49(1)	O5D−Fe1D−O6D	87.24(1)
O2C−Fe1C−O5C	88.68(1)	O2D−Fe1D−O5D	89.72(1)
O3C−Fe1C−N1C	76.34(1)	O3D−Fe1D−N1D	76.49(1)
O1B−Fe1C−O3C	92.76(1)	O1C−Fe1D−O3D	92.27(1)

Figure S10: Packing of **II** from left to right viewed down [100] and [001]. The hydrogen bond which links each tetramer to four others stabilises this formation. An undulating pattern can be seen along the a-b plane.

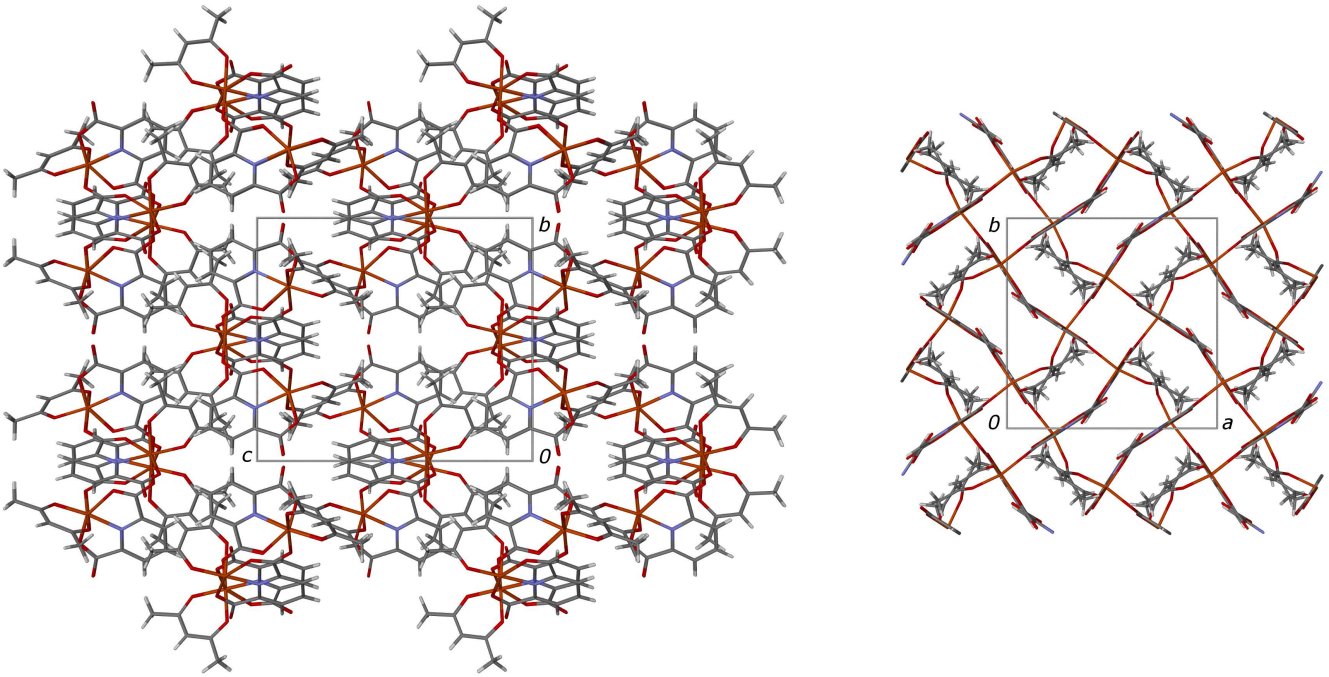

Figure S11: Packing of the tetramers of **III** with hydrogen bond stabilised layers viewed down [100]. Hydrogen atoms have been removed for clarity.

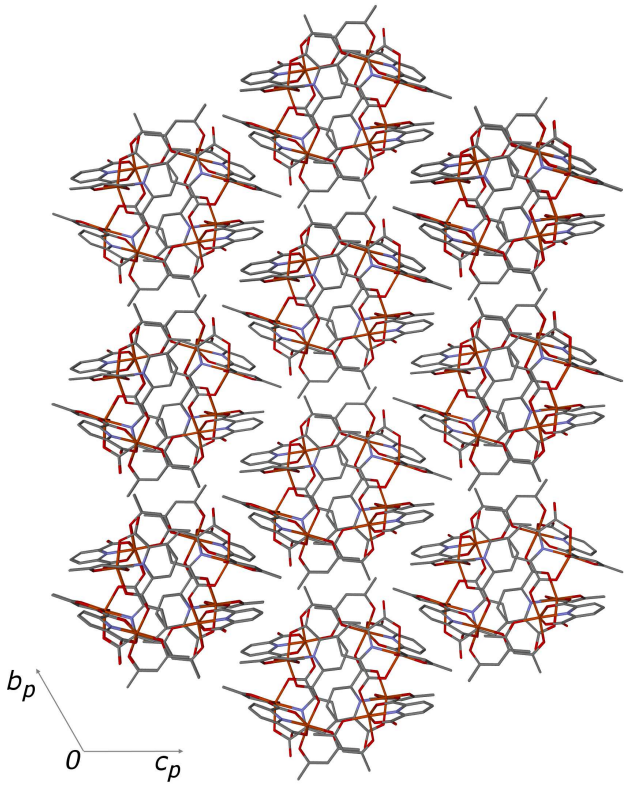

S3 Fourier transform-infrared spectroscopy

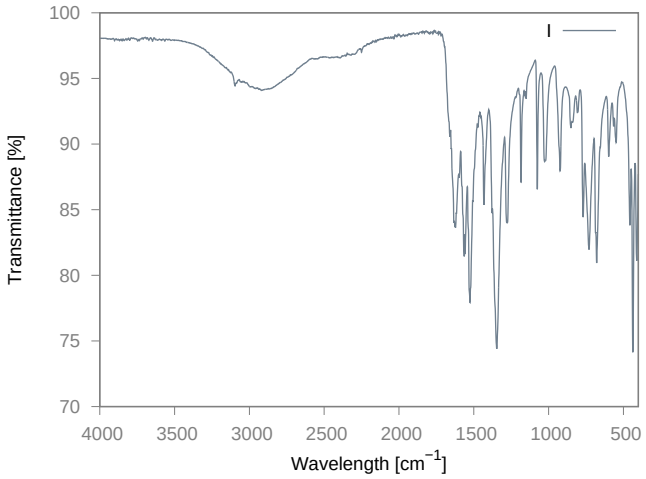

Figure S12: FT-IR spectrum of **I** grown at room temperature.

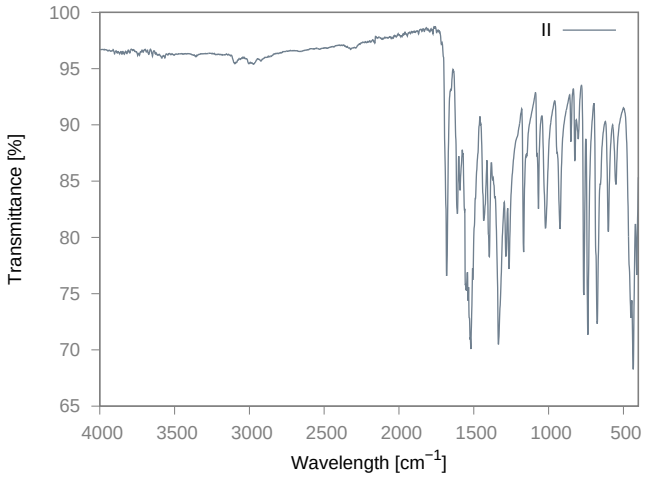

Figure S13: FT-IR spectrum of **II** grown at room temperature.

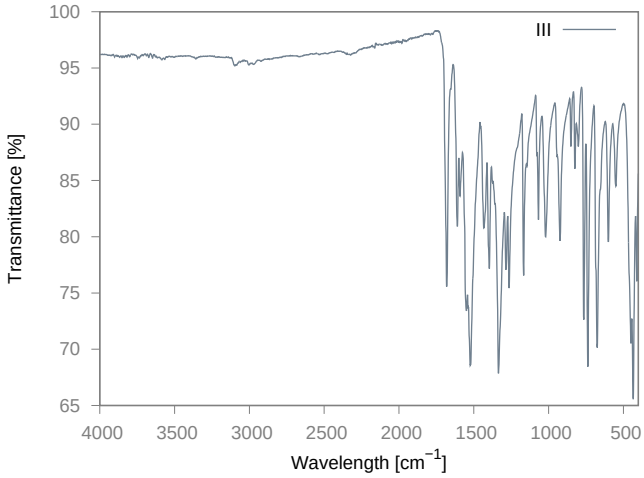

Figure S14: FT-IR spectrum of **III** grown at room temperature.